AIP | Journal of Applied Physics

Effects of plasma and vacuum-ultraviolet exposure on the mechanical properties of low-k porous organosilicate glass

X. Guo, J. E. Jakes, S. Banna, Y. Nishi, and J. L. Shohet

Citation: Journal of Applied Physics **116**, 044103 (2014); doi: 10.1063/1.4891501
View online: http://dx.doi.org/10.1063/1.4891501
View Table of Contents: http://scitation.aip.org/content/aip/journal/jap/116/4?ver=pdfcov
Published by the AIP Publishing

JOURNAL OF APPLIED PHYSICS **116**, 044103 (2014)

Effects of plasma and vacuum-ultraviolet exposure on the mechanical properties of low-k porous organosilicate glass

X. Guo,[1] J. E. Jakes,[2] S. Banna,[3] Y. Nishi,[4] and J. L. Shohet[1]
[1]*Plasma Processing & Technology Laboratory and Department of Electrical and Computer Engineering, University of Wisconsin-Madison, Madison, Wisconsin 53706, USA*
[2]*Performance Enhanced Biopolymers, USDA Forest Service Forest Products Laboratory, Madison, Wisconsin 53726, USA*
[3]*Applied Materials, Sunnyvale, California 94085, USA*
[4]*Stanford University, Stanford, California 94305, USA*

(Received 7 April 2014; accepted 16 July 2014; published online 29 July 2014)

The effects of plasma exposure and vacuum-ultraviolet (VUV) irradiation on the mechanical properties of low-*k* porous organosilicate glass (SiCOH) dielectric films were investigated. Nanoindentation measurements were made on SiCOH films before and after exposure to an electron-cyclotron-resonance plasma or a monochromatic synchrotron VUV beam, to determine the changes of film hardness, elastic modulus, and crack threshold due to these exposures. This permits the effects of ion bombardment and photon bombardment to be analyzed separately. The role of energetic ions was examined with a variety of inert plasma-exposure conditions. The role of VUV photons was analyzed as a function of synchrotron photon energy. It was found that both energetic ions and VUV photons with energies larger than the bond energy of the Si-O bond cause a significant increase in film hardness along with a smaller increase in elastic modulus and crack threshold. Differential Fourier transform infrared spectra and x-ray photoemission spectroscopy results show that the energetic ions affect the SiCOH properties mainly through physical bombardment, during which the ions transfer their momentum to the Si-O-Si backbone and transform them into more energetically stable Si-O-Si network structures. This results in the Si-O-Si network structures becoming densified. VUV photons assist reaction that increase the number of bridging $O_3\equiv$Si-O-Si$\equiv O_3$ bonds and deplete nonbridging $O_3\equiv$Si-O and C-Si$\equiv O_3$ bonds. This increased degree of cross linking in porous organosilicate dielectrics can substantially enhance their hardness and elastic modulus while showing no significant film shrinkage or densification.
[http://dx.doi.org/10.1063/1.4891501]

I. INTRODUCTION

Interconnect resistive-capacitive (RC) delay is a major challenge for the further continuous downscaling of integrated circuits. To reduce the capacitance, materials with ultralow dielectric constants are required in back-end-of-line (BEOL) integration, replacing conventional SiO_2 as inter-metal dielectrics.[1–3] Currently, two approaches are used to reduce the *k*-value of interconnect dielectrics: (1) reduction of the polarizability by increasing the level of low-polar bonds, mainly carbon-containing components (such as C-C, C-H, Si-CH_3, etc.) and/or (2) reduce the density by introducing porosity.[4] Normally, these low-*k* dielectrics possess poor mechanical properties as compared to SiO_2 and are vulnerable to plasma exposure during fabrication.[5] The presence of energetic ions, electrons, highly reactive radicals, and photons (from the deep vacuum ultraviolet (VUV) to the infrared (IR) range) can easily modify the chemistry of the carbon-containing components in these porous low-k dielectrics, and the porosity increases the reactivity and penetration depth of reactive species.[5]

Moreover, from the integration point of view when ultra low-*k* dielectrics are used, the mechanical strength is critical to sustain a downward force under chemical-mechanical planarization (CMP) processing of a large number of interconnect layers stacked together. Usually, the microprocessor unit (MPU) has more than 20 layers of interconnects,[6] and thus the dielectrics can be repeatedly exposed to plasma during fabrication. Modification of the chemistry of the dielectrics by plasma will affect their mechanical strength and will worsen the device reliability.

As a result, plasma-processing-induced damage has become a crucial impediment to successful integration of low-*k* dielectrics into integrated circuits and has generated extensive interest in studying the mechanisms that produce plasma damage in porous low-k dielectrics. Previous work has demonstrated that plasma exposure can affect the breakdown voltage, leakage current, capacitance,[7,8] and the time-dependent dielectric breakdown lifetimes of these materials.[9] In addition, the potentially large fluxes of energetic photons, particularly in the VUV range, have been shown to cause a number of unwanted effects, including differential charging of patterned structures,[10] and the creation of bulk and interfacial trap states that contribute to damage induced by leakage currents.[11] Additionally, recent work has reported that plasma exposure can adversely change the mechanical properties of low-*k* dielectrics, which will worsen dielectric reliability and degrade device performance.[12,13] Our previous work studied the effect of water uptake on the mechanical properties of these low-*k* dielectrics.[14]

However, the current understanding of plasma-induced mechanical property changes is still limited. The reports of dominant mechanisms of plasma-induced mechanical properties changes are not consistent. For example, Vanstreels[12] investigated the modification of He/H_2 plasma exposure on SiCOH low-*k* films and concluded that He/H_2 plasma exposure results in a decrease in both film hardness and elastic modulus because of plasma removal of porogen residues. In another study, Broussous[13] observed increases in both hardness and elastic modulus of SiCOH low-*k* films after He plasma exposure and attributed the changes to subsurface densification and/or structural modifications. Furthermore, few works have distinguished the roles of energetic ions and VUV photons when examining the effects of plasma exposure on the mechanical properties of low-*k* materials. The effects of charged-particle bombardment and photon irradiation are not yet fully elucidated.

Another concern is the change in mechanical properties as a function of VUV photon energy for VUV-irradiated low-*k* dielectrics, as compared with the changes developed during commonly used UV curing. UV-assisted curing with monochromatic or broadband light sources has been demonstrated to strengthen organosilicate interlayer dielectric thin films by significantly increasing their elastic modulus, hardness, and interfacial fracture energy while inducing relatively minor increases in dielectric constant and film density.[15,16] The structure of organosilicate dielectrics changes with increasing cure time, which is marked by the removal of terminal organic groups and increased network-forming bonds following the initial removal of porogen material. Recent studies[17] show that the UV-curing wavelength has a strong impact on the physical-chemical properties of low-*k* material. In particular, 172-nm UV photons induce greater changes to most of the film properties compared with a broadband UV light source.[17] On the other hand, the effect of the VUV irradiation wavelength on low-k dielectric material properties has received only minimal attention.

Thus, the object of this work is to investigate the separate effects of energetic charged-particles and vacuum-ultraviolet (VUV) photons during plasma processing on the mechanical properties of porous low-k organosilicate dielectrics (SiCOH). To determine this, nanoindentation measurements were made after exposure to plasma or VUV photons on a variety of samples to investigate the changes in their mechanical properties, including hardness (H), elastic modulus (E_s), and crack threshold (C_T). The role of charged-particle bombardment was examined under a variety of inert plasma-exposure conditions, which were specifically chosen to minimize the introduction of chemically reactive species. The roles of VUV photons were further isolated by choosing different photon energies under synchrotron radiation.

The nature of damage to porous SiCOH films for various exposures was analyzed using x-ray photoemission spectroscopy (XPS) and Fourier transform Infrared spectroscopy (FTIR). This provided direct information on how ion bombardment and/or photon irradiation affect the mechanical properties of porous low-k SiCOH films. The relationship between the changes in mechanical properties and photon energy was examined by exposing samples to monochromatic synchrotron radiation with specified photon energies.

II. EXPERIMENTAL DETAILS

The dielectric films used in this work are 640-nm low-*k* porous SiCOH that were plasma-enhanced chemical-vapor-deposited (PECVD) on $\langle 100 \rangle$ *p*-type silicon wafers. The deposition took place in a capacitively coupled PECVD reactor utilizing a 13.56 MHz radio frequency (RF) source in the presence of several inert and reactive gases with an organosilane precursor. Neither structure-forming techniques nor the introduction of porogen molecules were used in the deposition process. The dielectric constant (k) of the as-deposited material was measured to be 2.65 using capacitance-voltage (C-V) characteristics. After deposition, some of the films were UV cured using a Novellus Systems SOLA® Ultraviolet Thermal Processing (UVTP) system. The UV photon energy was between 3.1 and 6.2 eV with a total fluence of approximately 1×10^{16} photons/cm^2. After UV curing, the dielectric thickness was measured to be 500 nm and the dielectric constant (k) was measured to be 2.55. The density and atomic composition of the dielectric thin films with and without UV curing are shown in Table I.

Plasma exposures were made in an electron-cyclotron-resonance (ECR) plasma reactor operating with a 400 W, 2.45 GHz microwave power source and 875 G magnetic field, as illustrated in Figure 1. The ECR reactor can work in a "downstream" style when using a single magnet coil closest to the microwave-transmission window.[18] The sample chuck was located approximately 30-cm downstream from the resonant layer and it can be biased using a 100 W RF source and an L-type matching network.[19] By varying the RF power, a DC bias in the range of 0 to -100 V can be placed on the sample chuck, through which control of the ion-impact energy from the plasma can be accomplished. During plasma exposure, the temperature of the dielectric film was monitored with a thermocouple connected to the back of the sample.

To fully understand the effects of VUV photon irradiation, monochromatic photon radiation exposure was made at the University of Wisconsin Synchrotron Radiation Center using an apparatus as illustrated in Figure 2. Detailed information is available in previous work.[20] Compared with UV curing, synchrotron VUV irradiation utilizes higher photon energies and is carried out at room temperature without any thermal effects. By selecting various photon energies and fluences, synchrotron VUV irradiation can mimic the VUV environment in a processing plasma while completely separating any damage effects of VUV radiation produced by

TABLE I. Film density and atomic composition of as deposited and UV-cured porous organosilicate dielectrics (SiCOH) investigated in this work.

		Ratios of peak areas via FTIR	
Material	Film density (g/cm^3)	$Si\text{-}CH_3/Si\text{-}O$	$CH_x/Si\text{-}O$
As-deposited	1.15	6.6	8.9
UV-cured	1.25	3.5	3.2

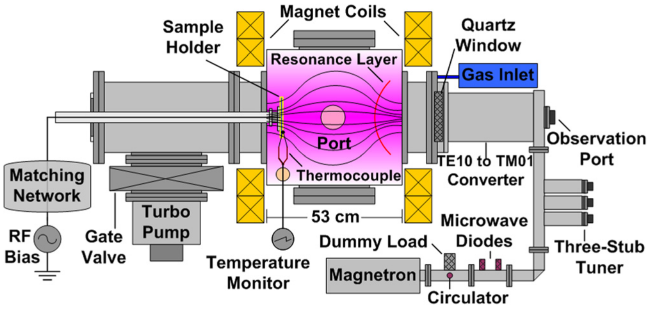

FIG. 1. Schematic of the electron cyclotron resonance plasma reactor apparatus used in this work.

charged-particle bombardment. Photon irradiation energies were specifically selected to mimic those emitted by processing plasmas: photons of 11.8 eV energy was used to mimic the strong VUV argon lines at 104.8 nm and 106.6 nm;[21] photons of 10.2 eV energy was used to mimic the CHF_3 (trifluoromethane, typically used feed gas for dielectric etch) discharge emitted strong VUV hydrogen line at 121.6 nm;[22] photons of 6.1 eV energy was used to mimic the C_2F_6 (hexafluoroethane, another typically used feed gas for dielectric etch) discharge emitted strong VUV carbon-fluorine line at 202.6 nm.[22] The temperature of the dielectric film under synchrotron radiation is also monitored with a thermocouple connected to the back of the sample.

After plasma or VUV exposure, nanoindentation tests were carried out on these low-*k* dielectrics using a Hysitron (Minneapolis, Minnesota, USA) TriboIndenter® equipped with a diamond Berkovich tip and operated in open-loop control. The machine compliance was evaluated using data from a series of indents with different loads placed in the center of a fused-silica standard and the SYS correlation.[23] Both calibration and SiCOH experiments utilized a load-control indent consisting of an initial 20 nm lift-off and reapproach in order to define the initial contact point accurately, followed by a 5 s loading, a 5 s hold at maximum load (P_{max}), a 2 s unloading to 40% of the P_{max}, a 60 s hold at 40% P_{max} to remove thermal drift effects, and a 1 s final unload. After correcting the fused silica load-depth traces for machine compliance, the series of indents were used to calculate the area function following the standard Oliver-Pharr method.[24] Film crack thresholds were also studied as described previously.[14] All the nanoindentation experiments were carried out at room temperature.

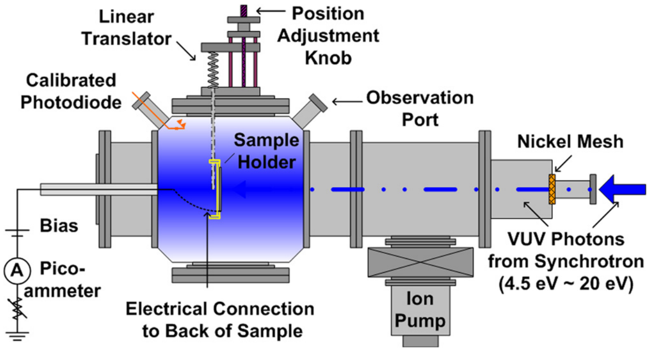

FIG. 2. Schematic of the synchrotron vacuum ultraviolet irradiation system used in this work.

It should be noted that, since the usual nanoindentation procedure relies on hardness (*H*) and elastic modulus (E_{eff}) readings generated by the nanoindentation instrument based on the penetration depth and indenter shape, the substrate of a thin film will have an increased effect on *H* and E_{eff} as the penetration depth increases. For thin films deposited on a hard substrate, as is the case of porous low-k films on a Si substrate, the results are usually overestimated and unconvincing if the effects of the hard substrate are not considered.[23] Also, for the porous structure of SiCOH, film densification underneath the probe could be significant during the indentation process, which brings additional challenges to nanoindentation analysis. To obtain more reliable testing, some necessary modifications were applied to the measured results, which have been discussed in detail in previous work.[14]

For chemical property measurements, FTIR and XPS were used. The film thickness and dielectric constant of the samples were measured using a three-color ellipsometer and C-V characteristics, respectively. The changes in elemental composition, chemical structures, thickness, and dielectric constant of the dielectrics for various exposure conditions were analyzed and compared.

III. RESULTS AND DISCUSSION

Table II summaries the changes in hardness (*H*), elastic modulus (E_s), and film crack threshold (C_T) after plasma or VUV exposure under varying conditions, in which the percentage changes of these properties were all calculated based on the pristine (no exposure) samples. We see that the film hardness (*H*), elastic modulus (E_s), and crack threshold (C_T) were obviously changed after plasma or VUV exposure. In this section, the roles of energetic charge-particles and VUV photons will be discussed separately.

A. Effect of energetic ions

To investigate the effects of plasma exposure on the mechanical properties in SiCOH during the plasma processing, both as-deposited SiCOH and UV-cured SiCOH films were exposed to various conditions. The ECR plasma reactor was operated in the "downstream" style, as described in Sec. II, for these exposures. Figure 3 illustrates the surface/bulk modification after plasma exposure of the dielectric films. To isolate the effects of energetic charged particles and photon bombardment from chemical changes due to reactive species, argon was used as the feed gas, under which the impact from reactive radicals is minimized.[18,19] This also excludes the impact from moisture uptake, since argon plasma, compared with O_2 plasma, does not change film hydrophobicity significantly.[14] The exposure time for each sample was set to be 5 min at 20 mTorr argon neutral pressure. The ion flux, measured using a Langmuir probe as described previously,[25] was determined to be 1.4×10^{14} ions/cm^2 s. The total ion fluence incident upon the sample surface is approximately 4.2×10^{16} ions/cm^2. The photon flux from the plasma was measured with a vacuum-ultraviolet monochromator over a

TABLE II. Changes in hardness (H), elastic modulus (E_s), and crack threshold (C_T) of the SiCOH films after argon plasma (ions and UV/VUV photons) or synchrotron (only UV/VUV photons) exposure of varied conditions.

Material	Exposure environment	Exposure conditions	% changes in hardness	% changes in modulus	% changes in crack threshold
As-deposited	Ions and UV/VUV photons	None	0	0	0
As-deposited		Plasma no bias	16 ± 1	4 ± 1	12 ± 2
As-deposited		Plasma −100 V bias	23 ± 1	6 ± 2	16 ± 2
UV-cured		None	0	0	0
UV-cured		Plasma no bias	9 ± 1	2 ± 1	8 ± 2
UV-cured		Plasma −100 V bias	14 ± 1	4 ± 2	10 ± 2
As-deposited	Only UV/VUV photons	6.1 eV	0 ± 1	0 ± 1	0 ± 2
As-deposited		10.2 eV	11 ± 1	3 ± 1	9 ± 2
As-deposited		11.8 eV	12 ± 1	4 ± 1	8 ± 2
As-deposited		8.0 eV	1 ± 1	0 ± 1	0 ± 2
As-deposited		8.5 eV	8 ± 1	3 ± 1	6 ± 2

range of wavelengths from 50 to 300 nm. The time-integrated photon fluence during the plasma exposure was in the order of 10^{15}–10^{16} photons/cm^2.

As shown in Figure 3, the energetic ions from the plasma collide with the dielectric surface and physically bombard the backbone bonds. The ion energy, controlled by the RF bias, varies from several electron volts to one hundred electron volts and the penetration depth of them normally will be no more than 2 nm.[26] The penetration distance of photons from an argon plasma into porous SiCOH films is close to 100 nm and appears to increase, based on simulation results, with photon fluence.[27] It has been reported that the ion-densification layer in these dielectric films, which is a layer underneath the sample surface in which density has increased from physical ion bombardment, is much larger than the distance ions can penetrate into the films: the ion-penetration depth. Thus, energetic ions can change the "bulk" film properties. The ion densification layer was observed to be about 30 nm for the plasma-exposed sample.[28] The mechanisms of these energetic-ion-induced "bulk" property changes will be analyzed in detail in the following.

During plasma exposure, the sample temperature was determined to increase from 22.5 °C to 39.8 °C after a 5-min exposure at 20 mTorr argon neutral pressure and 400 W microwave power. Compared with typical temperatures obtained during wafer fabrication including UV curing, the thermal-heating effect from plasma exposure is not enough to cause chemical bond changing within the sample, and will therefore be neglected. After exposure, the samples were kept in vacuum packaging and then were placed in the nano-indenter for testing. As illustrated in Table II, after plasma exposure (floating bias), for an as-deposited SiCOH film, there was a 16% increase in hardness, a 4% increase in modulus, and a 12% increase in the crack threshold, compared with that for an unexposed sample. For a UV-cured SiCOH, the plasma-exposed sample showed a 9% increase in hardness, a 2% increase in modulus, and an 8% increase in crack threshold, compared with the unexposed sample. These results indicate that plasma exposure can improve the mechanical properties of SiCOH by enhancing the hardness and elastic modulus. The smaller observed changes in the mechanical properties of UV-cured samples from plasma exposure are as a result of the mechanical strengthening induced by UV-curing.[15,16]

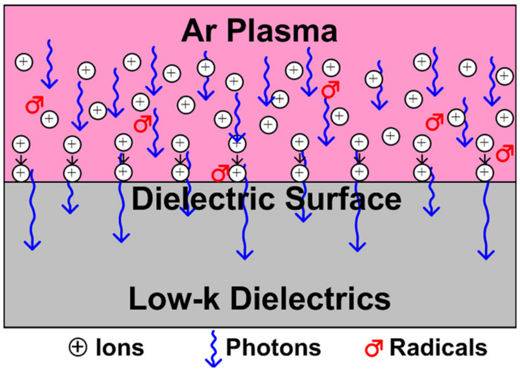

FIG. 3. Schematic drawing of surface/bulk modification effect of argon plasma on the dielectric films.

The differential FTIR spectrum was observed on an as-deposited SiCOH film after Ar plasma exposure by subtracting the spectrum of the pristine film from that of the plasma-exposed film. These results show that the improved mechanical properties are related to the plasma-induced bond rearrangement in the film. As shown in Figure 4, after plasma exposure, the bond intensities of the Si-O-Si network (~1063 cm^{-1}), Si-O-Si cage (~1130 cm^{-1}), and H-Si-O (890–990 cm^{-1}) were found to increase while those of the Si-(CH$_3$)$_n$ (1250–1280 cm^{-1}, 760–870 cm^{-1}) and the Si-O-Si suboxide (~1023 cm^{-1}) structures decreased. These differential FTIR results agree with those observed by Shi *et al.*, showing a significant methyl depletion and a pronounced enhancement of the Si-O-Si network bond structure.[28]

It should be noted that these bonding configuration changes are due to a synergy between the effects of energetic charged particles and VUV photons from Ar plasma.[21] Prager *et al.*[29] pointed out that energetic UV/VUV photon irradiation can depopulate the Si-O-Si cage bond (in which the Si-O-Si bond angle is approximately 150°) by forming more energetically stable Si-O-Si network bonds (Si-O-Si bond angle is 144°). However, our FTIR results show an *increased* Si-O-Si cage-bond intensity. Therefore, it can inferred that bombardment of energetic ions induces film-surface densification and is responsible for the increased Si-O-Si cage-bond density in the film surface, even though the

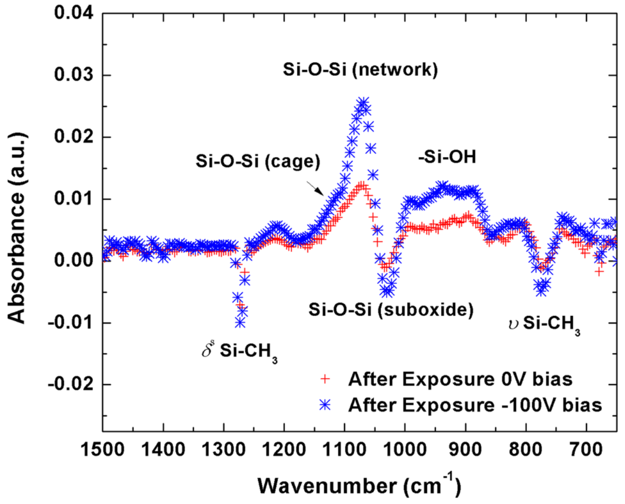

FIG. 4. Differential FTIR spectrum of plasma-exposed porous organosilicate dielectric films with floating potential or a -100 V DC bias applied to the sample chuck. Here, "δ^S" corresponds the bending vibrational mode and "υ" corresponds the stretching vibrational mode.

total number of these bonds over the entire volume of the film is reduced by VUV photon.[29,30]

To confirm this hypothesis, a -100 V_{DC} bias was applied to the sample chuck by varying the RF bias power. The sample was exposed to the same plasma conditions. The exposed time was also set to 5 min. Because all of the other plasma parameters remained unchanged, and because the steady-state RF bias does not draw a net DC current from the plasma, variation of the wafer bias should only change the energy of the ions impinging on the surface of the sample. In this case, we found that for as-deposited SiCOH films, the hardness increased by 23%, the modulus increased by 6%, and the crack threshold increased by 16%. Compared with the unexposed samples, the film hardness and crack threshold exhibited a significant increase. The modulus of the exposed sample shows a similar trend but lesser effect. For UV-cured SiCOH films, the hardness increased by 14%, the modulus increased by 4%, and the crack threshold increased by 10%, as shown in Table II. In the case of the modulus measurements, more than 30 points on the plasma-exposed sample were analyzed and each point was tested using the same loading function.[14] Including the effects of errors in the measurement, the change in modulus was $4 \pm 2\%$.

Differential FTIR spectra of plasma exposed film under -100 V_{DC} bias are also shown in Figure 4. Here, higher peaks of the Si-O-Si network ($\sim$1063 cm^{-1}), Si-O-Si cage ($\sim$1130 cm^{-1}), and open chain siloxanes H-Si-O (890–990 cm^{-1}) along with increased methyl depletion are seen compared with plasma exposure with no bias on the sample (floating). It should be noted that after plasma treatment, to minimize sample exposure to ambient air, they were sealed and kept in vacuum packs. The FTIR measurements were made in a chamber filled with dry N_2, to minimize oxidation of the plasma-damaged layer during the measurements. With regards to the possibility of the quartz window releasing oxygen during discharge, a residual gas analyzer (RGA) was used to examine the residual gas in the exposure chamber before and after the argon discharge. No additional oxygen was detected after the discharge. One plausible explanation for the increased number of Si-O bonds in SiCOH after Ar-plasma exposure is that the carbon atoms in the sample, existing in the C-O/H bond state, were sputtered away by the energetic ions. The residual O dangling bonds then reacted with Si dangling bonds to form open-chain siloxanes (HSi-O-SiH). This will be further discussed in the paragraph describing the XPS results.

When there was no bias, the sample surface had a floating potential near zero and the typical energy of ions that reached the film surface was relatively low (10 to 40 eV).[31] In contrast, under -100 V DC bias, the ion bombardment energy was more than one-hundred eV. These higher-energy ions can induce film densification in three ways:[32] First, physical bombardment of ions transfers their momentum to the Si-O-Si backbone structures and densifies them. Second, densification of the Si-OH bonds induces film shrinkage. Third, impurity radicals/ions in the argon plasma can react with the -Si-CH_3 groups on the porosity walls and can induce a collapse of the pore structures.[32] The first proposed mechanism leads to higher bond densities of the Si-O-Si network and Si-O-Si cage as seen in the differential FTIR results. The second mechanism results in an increased density of Si-OH bonds and the third mechanism is based on impurity induced methyl depletion. The reactive and oxidizing impurity gas mixed in argon, like O_2, results in a breaking of the Si-CH_3 bonds and removes -CH_3 from the centered Si atom.[5,30] RGA had been used to examine the vacuum integrity of the plasma vacuum chamber before each exposure. It shows that the pumping system worked well and no leaks were detected. The purity grade of the argon gas is "Research Grade." Thus, the possibility of chamber leaking and impurity from feed gas is minimal and was not seen on the residual gas analyzer, and we can safely neglect the third mechanism.

To figure out the dominant mechanism of ion induced film densification, XPS was performed on as-deposited SiCOH before and after plasma exposure. Figure 5 shows the O 1s, C 1s, and Si 2p electron orbital XPS spectra. The results for unexposed as-deposited sample show that the O 1s, C 1s, and Si 2p spectra consist of major peaks centered at approximately 531.8 eV, 284.1 eV, and 101.8 eV, respectively. The bond state is identified by fitting the spectra with a number of Gaussian peaks. As is shown in Figure 5, the Si 2p electron orbital spectrum consists of two peaks, which can be assigned to the C-Si-O_3 bond (101.4 eV)[33] and Si-Si-O_3 bond (102.5 eV).[34] The relative area of the C-Si-O_3 bond (65.2%) is about two times larger than that of Si-Si-O_3 bond (34.8%). The C 1s related peaks can be assigned to the C-O/H bonds (284.2 eV)[33] and O=C bonds (288.0 eV), and the relative area of the O=C bonds is estimated 5.2% approximately. The O 1s electron orbital spectrum has a major peak centered at 532.5 eV (O-Si related bonds) and a small peak centered at 530.6 eV (O-C bond).[35]

In the plasma-exposed samples, several changes were observed to these spectra. The intensity of the C 1s peak decreases after plasma exposure and the decrease is more significant in the -100 V_{DC} biased sample, indicating that energetic ions with higher energy (-100 V biased) can

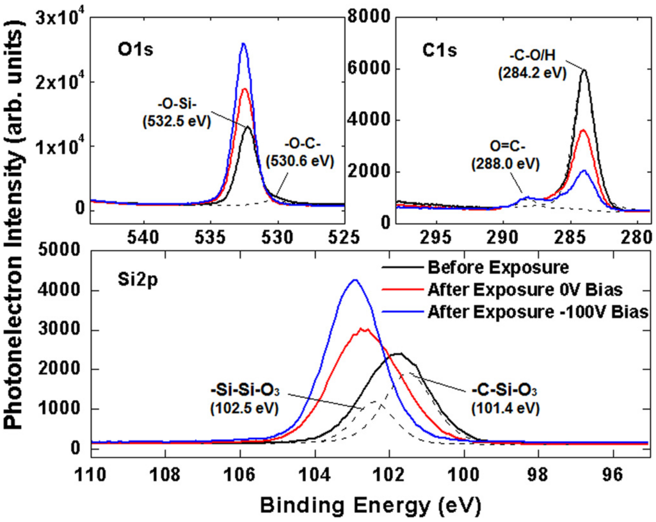

FIG. 5. XPS spectra showing the changes of O 1s, C 1s, and Si 2p electron orbitals of as-deposited samples after plasma exposure with floating potential or a -100 V DC bias applied to the sample chuck. The dashed lines are the deconvolution results after fitting the spectrum with the Gaussian peaks of the unexposed samples.

sputter away carbon more effectively. This is consistent with the -CH_3 peak decreasing in the FTIR results as described in the former part of this paper. XPS results show that the C 1s peak decreases mainly from the depletion of the C-O/H bonds at 284.2 eV. The damaged C-O/H bonds leave O dangling bonds in the film, which can react with other active bonds in the film, i.e., Si dangling bonds. In addition, the peak of the O 1s electron-orbital spectrum shifts slightly after plasma exposure. By selecting a pass energy of 10 eV with a corresponding absolute resolution <0.5 eV,[19] the peak shifted from 531.8 to 532.5 eV. Deconvolution via fitting the data with Gaussian peaks shows this small shift comes from the decrease of the O-C bonds (530.6 eV) produced by carbon depletion. The -100 V_{DC} bias plasma-exposed sample also shows a higher O 1s peak intensity. The peak of the Si 2p electron orbital spectrum has a significant shift to higher binding energies. For an unbiased plasma exposed sample, the Si 2p peak center moves to 102.8 eV. Deconvolution results show the Si-O_4 bond (103.0 eV), as well as the Si-O_3 bond (101.4 eV) and the Si-Si-O_3 bond (102.5 eV) are formed on the sample surface. As illustrated before, these changes are most likely a synergy of energetic ions and VUV photons in the plasma. For a -100 V_{DC} biased plasma-exposed sample, the Si 2p electron orbital spectra have a perfect Gaussian-shape peak centered at 103.0 eV (Si-O_4 bond) with a full width at half maximum (FWHM) of 1.81 eV, indicating that a Si-O-Si network-structure layer is formed at the sample surface. In addition, a significantly increased intensity of the Si 2p spectrum is seen, which indicates densification of the film surface.

Based on both FTIR and XPS results, it can be concluded that energetic ions can affect the SiCOH properties mainly through physical bombardment, during which the ions transfer their momentum to the Si-O-Si backbone and transform them to more stable Si-O-Si network structures. In the meanwhile, the concentration of the Si-O-Si network structures is increased. The mechanism for ion bombardment-induced film bulk densification is illustrated in Figure 6. Recall that surfaces exposed to an ECR plasma, working in a "downstream" configuration,[18] are subjected to bombardment by energetic ions, whose kinetic energy can vary from a few eV to hundreds of electron volts by controlling the sample RF bias.[19] Ion bombardments of this nature have very significant effects on the properties of the deposited film: when a high-energy ion strikes the surface, it can transfer its momentum to the Si-O-Si backbone structures (the matrix structure unit as shown in Figure 6) near the surface.[32] Since the backbone structures are cross-linked in the SiCOH film, the momentum can be transferred between the neighboring atoms/molecules. The "bulk" densification effects arise from a collision cascade which is induced by the continuing physical bombardment of ions.[36] Thus, any "spaces" under the surface atoms will tend to be filled in. Increasing ion bombardment tends to make films denser and cause the film to become more compressive.[37] Using an x-ray reflectivity (XRR) fitting based on multiple layer structures, Shi *et al.* reported a "bulk" densified layer of 30 nm in plasma-exposed ultra low-k dielectric film (k ~ 2.2) with the film density increasing by 20%, compared to the undensified layer at the film bottom.[28]

B. Effects of VUV photons

To better understand the observed results from plasma exposure, and to separate the effects of VUV photon bombardment from ion bombardment, monochromatic synchrotron VUV exposures were made on as-deposited SiCOH films. Photon-bombardment energies were specifically selected to be 6.1 eV, 10.2 eV, and 11.8 eV to mimic those emitted by C_2F_6, CHF_3, and Argon plasma. For each irradiation, the exposure times were chosen so that the total photon fluence impinging on the sample was the same (approximately 4.0×10^{15} photons/cm^2). This fluence is comparable to the total UV/VUV photon fluence emitted during the "downstream" ECR plasma exposure used in this work. The sample temperature did not show significant changes during synchrotron VUV irradiation.

The effects of VUV irradiation on the mechanical properties (film hardness, elastic modulus and crack threshold) of

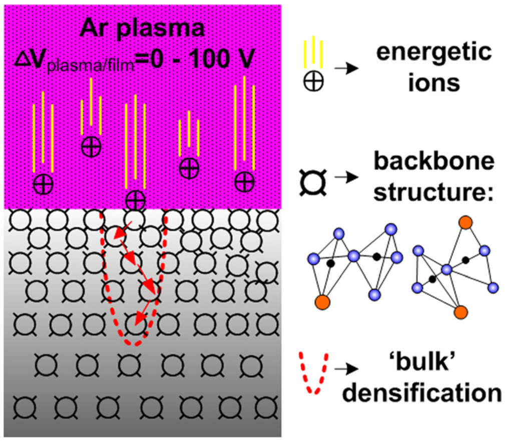

FIG. 6. Model of physical ion bombardment induced film bulk densification.

as-deposited porous SiCOH films are also summarized in Table II. It is observed that VUV photon irradiation with energies of 10.2 and 11.8 eV increases the film hardness by 11% and 12%, respectively, and increases the film elastic modulus by 3% and 4%. For the crack threshold, as defined in Sec. II, increases of 9% and 8%, respectively, were observed for these samples. These results are consistent with the results reported by Tatsumi *et al.*[38] that showed that the O-Si-O structure can be disordered by exposure to VUV radiation with energy of ∼10 eV or above. However, after additional irradiation with photons of energy 6.1 eV, the film hardness and modulus *were almost unchanged*. To confirm the existence of Si-O-Si, Si-C, and C-O/H bond states in the films after VUV irradiation with photons of various energies, FTIR and XPS measurements were made on the samples after each exposure.

The differential FTIR spectrum in Figure 7 shows that the bond densities of Si-$(CH_3)_n$ (1250–1280 cm^{-1}, 760–870 cm^{-1}), Si-O-Si cage (∼1130 cm^{-1}), and Si-OH (890–990 cm^{-1}) structures in as-deposited SiCOH films decreased significantly after VUV irradiation with photon energies of 10.2 and 11.8 eV and with a photon fluence of 4.0×10^{15} photons/cm^2. The peaks of the Si-O-Si network (∼1063 cm^{-1}) and the Si-O-Si suboxide (∼1023 cm^{-1}) structures *increased* after both 10.2 eV and 11.8 eV photon irradiation. These results indicate that a slight carbon loss and a structural rearrangement (i.e., conversion of the Si-O-Si bond from cage to network/suboxide resulting in a degradation of the Si-OH bonds).[29] However, for 6.1 eV photon-irradiated SiCOH films, only the bond densities of Si-$(CH_3)_n$ (1250–1280 cm^{-1}, 760–870 cm^{-1}) were found to decrease. Thus, these changes should be responsible for the mechanical property changes in the film.

Two mechanisms have been proposed for the degradation of Si-OH bonds by VUV photons in low-*k* films:[15,39] (a) a condensation reaction of two silanol groups, shown in Eq. (1), or (b) a photon-assisted reaction of one silanol and one methyl group, as shown in Eq. (2):

$$O_3 \equiv \text{Si-OH} + \text{HO-Si} \equiv O_3 \rightarrow O_3 \equiv \text{Si-O-Si} \equiv O_3 + H_2O, \tag{1}$$

$$O_3 \equiv \text{Si-OH} + H_3C\text{-Si} \equiv O_3 \rightarrow O_3 \equiv \text{Si-O-Si} \equiv O_3 + CH_4. \tag{2}$$

Since there is a significant loss of the -Si-CH_3 groups in the sample after VUV irradiation, as shown in the differential FTIR spectrum, it is tempting to view that reaction (2) is dominant in the context of the present study. The XPS spectra of the Si 2p, C 1s, and O 1s of the VUV exposed samples, as shown in Figure 8, support this argument. Compared with the unexposed sample, the ratio of the decreased area of the C 1s electron orbital XPS spectra to the increased area of the Si-O-Si peak (103 eV) in the 10.2 eV and 11.8 eV photon irradiated samples is approximately 0.8, illustrating that mechanism (2) dominates the reaction and is more active than mechanism (1). In addition, the peak area of the O 1s electron orbital XPS spectra of the samples after photon irradiation almost is almost same as that of the unexposed samples, which also shows mechanism (2) is dominant since mechanism (1) is oxygen-consuming. This photon-assisted reaction, illustrated by Eq. (2), increases the number of bridging $O_3{\equiv}$Si-O-Si$\equiv O_3$ bonds by depleting the nonbridging $O_3{\equiv}$Si-O and C-Si$\equiv O_3$ bonds, which further enhances the degree of crosslinking in the films.

Both the FTIR and XPS results show that no significant changes happen to the 6.1 eV photon-irradiated SiCOH, compared with an unexposed sample. This is the case even through an energy of 6.1 eV is higher than the bond strength of the C-Si bond, whose dissociation energy is 4.5 eV.[25] Prager *et al.*[29] pointed out that only VUV irradiation with wavelengths less than 190 nm ($E_{photon} > 6.5$ eV) can break the H_3C-Si bonds and generate Si-centered radicals which subsequently attract protons from neighboring groups. This explains why there is no experimentally observed mechanical property change in SiCOH after exposure to 6.1 eV photons.

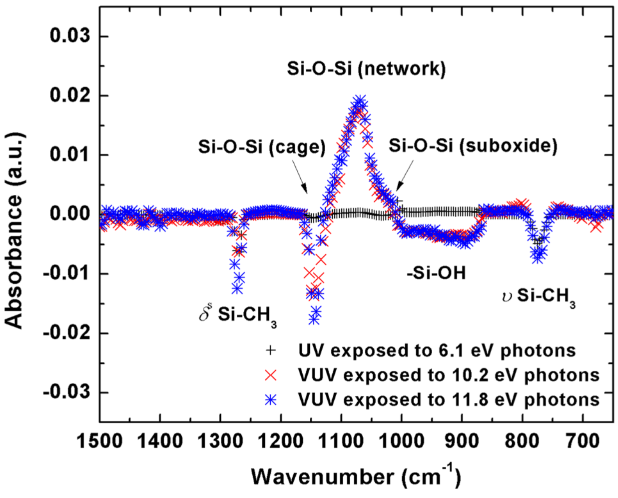

FIG. 7. Differential FTIR spectrum of porous organosilicate dielectric irradiated by synchrotron with several photon energies. Here, "δ^S" corresponds the bending vibrational mode and "υ" corresponds the stretching vibrational mode.

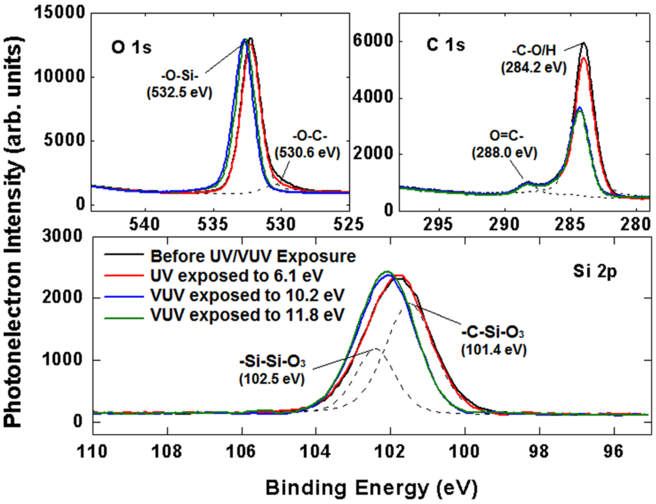

FIG. 8. XPS spectra showing the changes of O 1s, C 1s, and Si 2p electron orbitals of as-deposited samples after synchrotron irradiation several different photon energies. The dashed lines are the deconvolution results after fitting the spectrum with the Gaussian peaks of the unexposed samples.

To further check whether there is a critical VUV photon energy to trigger the reaction of generating the bridging $O_3{\equiv}Si\text{-}O\text{-}Si{\equiv}O_3$ bonds, 8.0 eV VUV photons, a little lower than the Si-O bond energies of (8.3 eV) and photons of 8.5 eV, a bit higher than the Si-O bond energy, with the same fluence, were used to irradiate the sample. It was found that after 8.0 eV photon irradiation, no obvious changes in film hardness, modulus, and crack threshold were observed, just as in case of the 6.1 eV photon-irradiated sample. However, after 8.5 eV photon irradiation, the film hardness was found to increase 8% and the elastic modulus and crack threshold increased 3% and 6%, respectively, which is comparable to that found for 10.2 and 11.8 eV photon-irradiated samples.

It also has been reported that if large angle Si-O-Si bonds (>144°, i.e., Si-O-Si cage) and structural imperfections are present in organosilicate glass films, deep UV radiation with a wavelength smaller than 150 nm ($E_{photon} > 8.26$ eV) on these films can induce a structural rearrangement by converting the existing silica bonds into small angle Si-O-Si bonds (Si-O-Si network).[15,29] This structural rearrangement can be only initiated by UV/VUV irradiation with shorter wavelengths than the absorption edge of the Si-O-Si network. This threshold of photon energy coincidentally corresponds with the Si-O bond strength (8.3 eV). This is confirmed by analysis of the FTIR spectrum of the VUV photon-irradiated samples, as shown in Figure 7. The structural rearrangement occurs in 10.2 and 11.8 eV photon-irradiated samples but hardly at all in 6.1 eV photon-irradiated samples. Only photons with energy larger than the Si-O bond energy (8.3 eV) can trigger the silica-bond conversion: from Si-O-Si cage to Si-O-Si network. Of the two bond states, the latter is more energetically stable than the former. Thus, the film mechanical properties can benefit from the increasing of energetically stable network structure within the film. It should be noted that no significant compositional change or film densification is observed in this progress. This is quite different from the plasma induced Si-O-Si structural rearrangements. The peak shift of the Si 2p electron orbital XPS spectra of the 10.2 and 11.8 eV photon-irradiated samples is attributed to the high binding energy of the Si 2p electrons, as shown in Figure 8, indicates the increase in the concentration of the $Si\text{-}O_4$ bond and the enhancement of the Si-O-Si network-structure layer at the surface. This further corroborates the proposed structural rearrangement generated within the dielectrics that converting the Si-O-Si bond from the cage configuration to a more energetically stable network configuration.

IV. CONCLUSIONS

Both plasma exposure and VUV photon irradiation were found to cause enhancement of SiCOH film mechanical characteristics, resulting in a significant increase in film hardness and crack threshold, and showing a smaller increase in elastic modulus. This work has separated the roles of energetic ions and VUV photons arising from plasma exposure. Differential FTIR spectra and XPS measurements show that the energetic ions can affect the SiCOH properties mainly through physical bombardment. The ions transfer their momentum to the Si-O-Si backbone to form more stable Si-O-Si network structures. VUV photon irradiation can enhance the hardness, elastic modulus, and also the crack threshold of the film but only when the photon energy is above the bond energy of Si-O. This latter enhancement comes from the photon-assisted reaction that increases the number of bridging $O_3{\equiv}Si\text{-}O\text{-}Si{\equiv}O_3$ bonds by depleting nonbridging $O_3{\equiv}Si\text{-}O$ and $C\text{-}Si{\equiv}O_3$ bonds, along with an increase in the degree of cross linking within the film. In addition, photons with energies higher than the Si-O bond energy can induce a pronounced conversion of the Si-O-Si bond from the cage configuration to a more energetically stable network configuration, with no significant compositional change or film densification occurs in this process.

ACKNOWLEDGMENTS

This work was supported by the Semiconductor Research Corporation under Contract No. 2012-KJ-2359 and by the National Science Foundation under Grant No. CBET-1066231 and by the Applied Materials University Research Partnership Program.

[1] K. Maex, M. R. Baklanov, D. Shamiryan, F. Iacopi, S. H. Brongersma, and Z. S. Yanovitskaya, J. Appl. Phys. **93**, 8793 (2003).
[2] M. R. Baklanov and K. Maex, Philos. Trans. R. Soc. London, Ser. A **364**, 201 (2006).
[3] A. Grill, J. Appl. Phys. **93**, 1785 (2003).
[4] A. Grill, "Low and ultralow dielectric constant films prepared by plasma enhanced chemical vapor deposition," in *Dielectric Films for Advanced Microelectronics*, edited by M. Baklanov, M. Green, and K. Maex (John Wiley & Sons, Ltd, Chichester, UK, 2007).
[5] M. R. Baklanov, J. F. de Marneffe, D. Shamiryan, A. M. Urbanowicz, H. Shi, T. V. Rakhimova, H. Huang, and P. S. Ho, J. Appl. Phys. **113**, 041101 (2013).
[6] R. H. Havemann and J. A. Hutchby, Proc. IEEE **89**, 586 (2001).
[7] J. Atkin, E. Cartier, T. Shaw, R. Laibowitz, and T. Heinz, Appl. Phys. Lett. **93**, 122902 (2008).
[8] J. Atkin, D. Song, T. Shaw, E. Cartier, R. Laibowitz, and T. Heinz, J. Appl. Phys. **103**, 094104 (2008).
[9] M. T. Nichols, H. Sinha, C. A. Wiltbank, G. A. Antonelli, Y. Nishi, and J. L. Shohet, Appl. Phys. Lett. **100**, 112905 (2012).
[10] S. Uchida, S. Takashima, M. Hori, M. Fukasawa, K. Ohshima, K. Nagahata, and T. Tatsumi, J. Appl. Phys. **103**, 073303 (2008).
[11] B. Jinnai, T. Nozawa, and S. Samukawa, J. Vac. Sci. Technol. B **26**, 1926 (2008).
[12] K. Vanstreels and A. M. Urbanowicz, J. Vac. Sci. Technol. B **28**, 173 (2010).
[13] L. Broussous, G. Berthout, D. Rebiscoul, V. Rouessac, and A. Ayral, Microelectron. Eng. **87**, 466 (2010).
[14] X. Guo, J. E. Jakes, M. T. Nichols, S. Banna, Y. Nishi, and J. L. Shohet, J. Appl. Phys. **114**, 084103 (2013).
[15] F. Iacopi, Y. Travaly, B. Eyckens, C. Waldfried, T. Abell, E. P. Guyer, D. M. Gage, R. H. Dauskardt, T. Sajavaara, K. Houthoofd, P. Grobet, P. Jacobs, and K. Maex, J. Appl. Phys. **99**, 053511 (2006).
[16] F. Iacopi, G. Beyer, Y. Travaly, C. Waldfried, D. M. Gage, R. H. Dauskardt, K. Houthoofd, P. Jacobs, P. Adriaensens, K. Schulze, S. E. Schulz, S. List, and G. Carlotti, Acta Mater. **55**, 1407 (2007).
[17] P. Marsika, A. M. Urbanowicz, P. Verdonck, D. D. Roest, H. Sprey, and M. R. Baklanov, Thin Solid Films **519**, 3619 (2011).
[18] M. T. Nichols, K. Mavrakakis, Q. Lin, and J. L. Shohet, J. Appl. Phys. **114**, 104107 (2013).
[19] M. T. Nichols, Ph.D. dissertation, University of Wisconsin-Madison, Madison, WI, 2013.
[20] J. L. Lauer, J. L. Shohet, and R. W. Hansen, J. Vac. Sci. Technol. A **21**, 1253 (2003).
[21] H. Ren, G. A. Antonelli, Y. Nishi, and J. L. Shohet, J. Appl. Phys. **108**, 094110 (2010).
[22] J. R. Woodworth, M. E. Riley, V. A. Amatucci, T. W. Hamilton, and B. P. Aragon, J. Vac. Sci. Technol. A **19**, 45 (2001).
[23] D. S. Stone, K. B. Yoder, and W. D. Sproul, J. Vac. Sci. Technol. A **9**, 2543 (1991).

[24] W. C. Oliver and G. M. Pharr, J. Mater. Res. **7**, 1564 (1992).

[25] H. Ren, Y. Nishi, and J. L. Shohet, Electrochem. Solid-State Lett. **14**, H107 (2011).

[26] W. M. Lau, I. Bello, L. J. Huang, X. Feng, M. Vos, and I. V. Mitchell, J. Appl. Phys. **74**, 7101 (1993).

[27] J. Shoeb, M. Wang, and M. J. Kushner, J. Vac. Sci. Technol. A **30**, 041303 (2012).

[28] H. Shi, H. Huang, J. Bao, J. Liu, P. S. Ho, Y. Zhou, J. T. Pender, M. D. Armacost, and D. Kyser, J. Vac. Sci. Technol. B **30**, 011206 (2012).

[29] L. Prager, P. Marsik, L. Wennrich, M. R. Baklanov, S. Naumov, L. Pistol, D. Schneider, J. W. Gerlach, P. Verdonck, and M. R. Buchmeiser, Microelectron. Eng. **85**, 2094 (2008).

[30] J. Bao, H. Shi, J. Liu, H. Huang, P. S. Ho, M. D. Goodner, M. Moinpour, and G. M. Kloster, J. Vac. Sci. Technol. B **26**, 219 (2008).

[31] J. Chen and Z. Ren, Vacuum **52**, 411 (1999).

[32] H. Cui, R. J. Carter, D. L. Moore, H. G. Peng, D. W. Gidley, and P. A. Burke, J. Appl. Phys. **97**, 113302 (2005).

[33] S. Y. Jing, H. J. Lee, and C. K. Choi, J. Kor. Phys. Soc. **41**, 769 (2002).

[34] T. P. Nguyen and S. Lefrant, J. Phys. Condens. Matter **1**, 5197 (1989).

[35] H. Kitoh, M. Muroyama, M. Sasaki, M. Iwasawa, and H. Kimura, Jpn. J. Appl. Phys., Part 1 **35**, 1464 (1996).

[36] R. H. Bassel, T. D. Andreadis, M. Rosen, G. P. Mueller, and G. K. Hubler, MRS Proc. **128**, 151 (1988).

[37] L. Cui, Ph.D. dissertation, University of Minnesota, Minneapolis, MN, 2013.

[38] T. Tatsumi, S. Fukuda, and S. Kadomura, Jpn. J. Appl. Phys. **33**, 2175 (1994).

[39] M. G. Albrecht and C. Blanchette, J. Electrochem. Soc. **145**, 4019 (1998).